National Marine Fisheries Service
NOAA

Fishery Bulletin
established in 1881

Spencer F. Baird
First U.S. Commissioner of Fisheries and founder of *Fishery Bulletin*

Bayesian estimation of the age and growth of the round stingray (*Urobatis halleri*) in the Gulf of California in Mexico

J. Fernando Márquez-Farías[1]
L. Daniel Carrillo-Colín[2]
Allan Rosales-Valencia[1]
Raúl E. Lara-Mendoza[3]
Oscar G. Zamora-García (contact author)[4]

Email address for contact author: ozamora@sirbaa.com

[1] Facultad de Ciencias del Mar
Universidad Autónoma de Sinaloa
Paseo Claussen s/n
Colonia Los Pinos
82000 Mazatlán, Sinaloa, Mexico

[2] Posgrado en Ciencias del Mar y Limnología
Universidad Nacional Autónoma de Mexico
Avenida Ciudad Universitaria 3000
04510 Coyoacán, Ciudad de Mexico, Mexico

[3] Dirección General Adjunta de Investigación Pesquera en el Atlántico
Instituto Nacional de Pesca y Acuacultura
Secretaría de Agricultura y Desarrollo Rural
Avenida Mexico 190
Colonia Del Carmen
04100 Coyoacán, Ciudad de Mexico, Mexico

[4] Servicios Integrales de Recursos Biológicos, Acuáticos y Ambientales
Avenida Macarela 3302
Edificio Cardones I-104
Palmilla Grand Residencial
82112, Mazatlán, Sinaloa, Mexico

Abstract—Life-history studies of species discarded in fisheries are a low priority, particularly those of age and growth estimation. Consequently, almost everything is unknown about such species despite their having been caught as bycatch over the long term. In this study, age estimates were obtained by using the vertebrae of round stingrays (*Urobatis halleri*). We fitted 3 different growth models (von Bertalanffy, Gompertz, and logistic) to length-at-age data. Bayesian estimation of the various growth parameters was done by using the Markov chain Monte Carlo algorithm. Prior distributions of the parameters disc width at birth (DW_0) and the theoretical maximum disc width (DW_∞) were included and considered informative. The priors for the growth coefficient (k) and the completion growth parameter (k_2) were set as noninformative (k for the von Bertalanffy growth function and k_2 for the Gompertz and logistic growth models). Results of our analyses indicate that growth bands are annual and that the round stingray lives up to 8 years. According to the Watanabe–Akaike information criterion for model selection, the von Bertalanffy growth function for sexes combined was selected as the best model. The mean values of marginal posteriors were as follows: DW_0=9.52 cm (95% credible interval [CI]: 9.25–9.79), DW_∞=32.50 cm (95% CI: 30.60–34.46), and k=0.114 year^{-1} (95% CI: 0.101–0.129).

Manuscript submitted 28 January 2022.
Manuscript accepted 9 June 2022.
Fish. Bull. 120:205–217 (2022).
Online publication date: 8 July 2022.
doi: 10.7755/FB.120.3-4.2

The geography and oceanographic characteristics of the Gulf of California (GOC) provide a highly productive area that supports some of the largest fisheries in Mexico. As a result, the GOC is one of the most productive regions for elasmobranchs. According to official fisheries statistics, in 2018, ~59% and ~39% of the landings of sharks and rays (batoids), respectively, came from the GOC (CONAPESCA[1]).

Both the industrial and artisanal fisheries of the GOC contribute to the landings of batoids (Márquez-Farías, 2002; Bizzarro et al., 2009). In addition to the current exploitation by industrial and artisanal ray fisheries, elasmobranch populations have been affected by the shrimp-trawl fishery that has been operating in the GOC since 1921 (Lluch-Cota et al., 2007).

The most important species in the landings of the ray fishery belong to the families Rhinobatidae, Dasyatidae, Myliobatidae, and Gymnuridae (Saldaña-Ruíz et al., 2016). In addition, because the fishing grounds of the artisanal ray fishery are inshore, the landings frequently include juveniles and pregnant females of many species (Márquez-Farías and Blanco-Parra, 2006; Bizzarro et al., 2009).

The composition of ray species in landings varies depending on the type of fishery, essentially because of the seasonal migrations of individuals, the habitat they occupy, and their susceptibility to capture. Given this situation and

[1] CONAPESCA (Comisión Nacional de Acuacultura y Pesca). 2018. Anuario estadístico de acuacultura y pesca 2018, 277 p. Comisión Nacional de Acuacultura y Pesca, Mazatlán, Mexico. [Available from website.]

the magnitude of the exploitation of elasmobranchs, the research priorities in the Mexican national plan of action for sharks focus on the more abundant species in the catch (CONAPESCA-INP, 2004). Considering the time series of historical catch of rays, the mixed-species fisheries, and the disadvantages of the low biological productivity of elasmobranchs (Musick, 1999), the negative effect of multiple fisheries on ray populations is presumably high.

A recent study of species composition and fishing dynamics revealed the effect of the industrial shrimp fishery on the elasmobranch populations of the GOC (Garcés-García et al., 2020). Results from that study confirm the importance of American round rays (family Urotrygonidae) as bycatch. The round stingray (*Urobatis halleri*) is the most abundant fish species in the bycatch of the industrial shrimp fishery in the GOC (López-Martínez et al., 2010; Rábago-Quiroz et al., 2011). Unfortunately, up to 95% of the bycatch volume of the shrimp fishery in the GOC is discarded at sea because of its low commercial importance (Zamora-García, 2015), limiting the study of the life history of the round stingray and other species.

The round stingray is distributed from California (in the United States) to Ecuador. It is a benthic and small (maximum disc width [DW]: 30.8 cm) batoid inhabiting soft mud or sand bottoms and is usually found in nearshore waters less than 15 m deep but can occur at depths down to 91 m (McEachran and Notarbartolo-di-Sciara, 1995). Aggregations are modulated by water temperature (>17°C) (Ebert, 2003; Hoisington and Lowe, 2005). Its food preferences include benthic invertebrates, bivalves, and small fishes. It is a viviparous species, and brood size ranges from 1 to 6 pups per season, depending on the size of the female (Babel, 1967), after 3 months of gestation (Nordell, 1994).

Differences in life-history traits in some elasmobranch species, such as the shovelnose guitarfish (*Pseudobatos productus*) and Pacific angel shark (*Squatina californica*), have been documented between populations in California and those farther south on the western coast of Baja California and in the GOC in Mexico (Márquez-Farías, 2007, 2020). The growth characteristics of round stingrays have been estimated for only the California population and are unknown for the GOC population (Hale and Lowe, 2008). The round stingray is categorized as a species of least concern in the IUCN Red List of Threatened Species (Lyons et al., 2015). From a regional perspective, populations of the round stingray and other rays likely have been affected by the shrimp-trawl fishery, given its intensity for more than 70 years in the GOC.

In this study, we report the results of Bayesian analyses used to investigate the age and growth of the round stingray in the GOC for the first time. First, using standard aging protocols, we used sectioned vertebrae to interpret and count the growth bands and to test the accuracy of band counts by readers. Then, we fitted 3 nonlinear growth models to age–length data pairs to estimate growth. Selection of the model that best explained and predicted the length-at-age data was based on the Watanabe–Akaike information criterion (WAIC), an appropriate approach for Markov chain Monte Carlo numerical integration. Growth parameters are presented as posterior probabilities that summarize the information of data and the prior probability of the parameters. The results of this study provide insight into key population characteristics necessary to model the demography of the round stingray and to test its potential resilience to fishing mortality.

Material and methods

Data and sample collection

Specimens of the round stingray were collected monthly during 2007–2012 as bycatch from trawl surveys conducted by the artisanal shrimp fishery in Teacapan, Sinaloa, Mexico (22°32′N, 105°45′W). We recorded the sex of each specimen and measured the DW (in centimeters) in a straight line, avoiding the curvature of the body. In addition, a section of 8–10 cervical vertebrae was extracted from each specimen to prevent intravertebral variability of band pairs (Natanson et al., 2018). Finally, the samples were labeled and frozen at –20°C at lab facilities for subsequent analysis.

Sample processing

Excess tissue and neural arches were removed from the vertebral segments manually. Each centrum was removed and mounted onto a flat piece of wood with synthetic resin. The vertebral diameters (VDs) were measured sagittally (to the nearest 0.05 mm) by using a Wixey[2] WR100 digital vernier (Barry Wixey Development, Seattle, WA). Using an IsoMet Low-Speed Saw (Buehler Ltd., Lake Bluff, IL), with twin blades separated by 0.24 mm, we cut each vertebra in a sagittal plane through the focus. Each vertebral section was mounted on a slide and photographed by using transmitted light with an Olympus SZ61 stereoscopic microscope (Olympus Corp., Tokyo, Japan) equipped with an Infinity*1-2* digital camera (Teledyne Lumenera, Ottawa, Canada). We created an image bank for the interpretation and counting of growth bands.

Size frequency and the relationship of size to vertebral diameter

We prepared DW–frequency histograms for comparison of size between the sexes. We used a *t*-test to determine whether there was a difference in the mean size between the male and female specimens. The relationship between VD and DW was assessed by using linear regression.

[2] Mention of trade names or commercial companies is for identification purposes only and does not imply endorsement by the National Marine Fisheries Service, NOAA.

Age estimation

In the vertebral sections of round stingrays, growth-band pairs appear opaque and translucent under transmitted light (Cailliet et al., 2006). Age estimates were made by counting band pairs along the corpus calcareum after identifying the birthmark, which can be seen as a change in the angle close to the focus. After establishing the aging criteria, 3 independent readers counted the growth bands.

Aging bias and precision

Reproducibility of counts of growth bands was assessed by using the index of average percent error (IAPE) (Equation 1) and the coefficient of variation (CV) (Equation 2). Next, the accuracy was evaluated by using the precision index (D) (Equation 3) for estimates from the 3 readers together and between readers (Chang, 1982; Goldman and Musick, 2006). Finally, the consensus of growth-band counts was visually evaluated by using age-bias plots (Campana et al., 1995). The following equations were used:

$$IAPE = 100\left[\frac{1}{\mathrm{N}}\sum_{\mathrm{j}=1}^{\mathrm{N}}\left(\frac{1}{R}\sum_{\mathrm{i}=1}^{\mathrm{R}}\frac{\left|x_{\mathrm{ij}}-\bar{x}_{\mathrm{j}}\right|}{\bar{x}_{\mathrm{j}}}\right)\right]; \quad (1)$$

$$CV = 100\left[\frac{1}{\mathrm{N}}\left(\sqrt{\sum_{\mathrm{i}=1}^{\mathrm{R}}\frac{(x_{\mathrm{ij}}-\bar{x}_{\mathrm{j}})^2}{R}}\right)\right]; \text{and} \quad (2)$$

$$D = \left[100\left(\frac{A}{B}\right)\right], \quad (3)$$

where N = the number of individuals aged;
R = the number of readers;
x_{ij} = the age estimate i for individual j;
$\bar{x}_{\mathrm{j}}$ = the mean age calculated for individual j;
A = the number of agreements; and
B = the number of readings done.

For further analyses, we considered only age estimates on which at least 2 readers agreed; otherwise, the reading was discarded (Goldman et al., 2012). After growth bands were counted, the radius (distance from the focus to the edge) of a vertebra and each band's thickness were recorded by using Image-Pro Plus image analysis software (vers. 6.0, Media Cybernetics Inc., Rockville, MD).

Periodicity of band formation

The periodicity of growth-band formation in round stingrays was assessed through centrum edge analysis (CEA) and marginal increment analysis (MIA) following Cailliet (2015). First, we categorized the edge type of each section of a vertebra as *opaque* or *translucent*. Then, the relative frequency of each edge type was tabulated in bimesters (2-month intervals). The MIA (Equation 4) was conducted bimonthly by using the ages 2–8 years, following Natanson et al. (1995). Bimesters with mean marginal increment (MI) values close to 1 were interpreted to be the time of year when the growth cycle is about to be completed (Cailliet et al., 2006):

$$MI = \left(\frac{VR - r_{\mathrm{n}}}{r_{\mathrm{n}} - r_{\mathrm{n-1}}}\right), \quad (4)$$

where VR = the vertebral radius;
r_{n} = the distance from the focus to the last band pair; and
$r_{\mathrm{n-1}}$ = the distance from the focus to the penultimate band pair.

One-way analysis of variance (ANOVA) was used to assess both the strength of the difference in total band counts between each pair of readers and the differences in the MI among bimesters (Gerrodette, 2011; Carrillo-Colín et al., 2021).

A Bayesian approach was used for the t-test, the linear regression, and the ANOVA described above. The Bayes factor (BF_{10}) was used to measure the weight of the evidence of the alternative hypothesis (H_1) against the null hypothesis (H_0) (Kass and Raftery, 1995; Rouder et al., 2009):

$$BF_{10} = H_1 / H_0. \quad (5)$$

The null hypothesis corresponds to the effect size (δ) of 0, and the alternative hypothesis was specified as a Cauchy prior with location and scale parameters of 0.000 and 0.707, respectively (Jeffreys, 1961).

All statistical treatments were done under the Bayesian approach by using the programs JAGS (vers. 4.3.0; Plummer, 2003) and JASP (vers. 0.15; JASP Team, 2021), statistical software R, vers. 4.0.5 (R Core Team, 2021), and the BayesFactor R package (vers. 0.9.12-4.2; Morey and Rouder, 2018). We relied on the guidelines proposed by Jeffreys (1961) for interpreting BF_{10}.

Growth modeling

To maximize the accuracy of the length-at-age predictions for both sexes of round stingrays and to contrast different hypotheses about growth, we used the von Bertalanffy, Gompertz, and logistic growth models (Katsanevakis and Maravelias, 2008). Growth models included in this study were those versions that incorporate disc width at birth (DW_0), as recommended for rays (Smart et al., 2016):
von Bertalanffy growth function (VBGF),

$$DW_{\mathrm{t}} = DW_{\infty} - (DW_{\infty} - DW_0)\mathrm{e}^{-\mathrm{kt}}; \quad (6)$$

Gompertz growth model,

$$DW_{\mathrm{t}} = DW_0\mathrm{e}^{-\log\left(\frac{\mathrm{DW_0}}{\mathrm{DW_\infty}}\right)\left(1-\mathrm{e}^{-\mathrm{k_2 t}}\right)}; \text{and} \quad (7)$$

logistic growth model,

$$DW_t = \frac{DW_\infty DW_0 e^{k_2 t}}{DW_\infty + DW_0 e^{k_2 t - 1}}, \quad (8)$$

where DW_t = the estimated disc width (in centimeters) at a given age t (in years);
DW_∞ = the theoretical maximum disc width (in centimeters);
k = the growth coefficient (year^{-1}); and
k_2 = the completion growth parameter (year^{-1}).

Model fitting was done by using the Bayesian approach, which requires an initial probability distribution (prior) for each model parameter. We conducted a meta-analysis based on growth parameters published in the literature for round stingrays (Table 1). The mean and standard deviation of published growth parameters were used to set the parameters of the prior distributions (informative). The priors for the parameters k and k_2 were chosen to be relatively noninformative as the uniform distribution, with a minimum of 0 and maximum of 10 to avoid negative values and let the model acquire the needed curvature (Smart and Grammer, 2021). The prior for DW_∞ was informative and set as a normal distribution (ND): the population mean equal to 33.05 (standard deviation [SD] 10.07). The prior for DW_0 was also informative with an ND (population mean=7.32, σ=0.29). The prior of the residual σ was uniform, with a minimum of 0 and a maximum of 100.

The posterior distribution for the parameters of the 3 growth models (Equations 6–8) was computed by using the Bayes theorem (Gelman et al., 2003). With the actual growth parameters substituted into the Bayes formula and the terms simplified, the equation is as follows:

$$P(DW_\infty, k_n, DW_0 | d) = \frac{P(d|DW_\infty, k_n, DW_0) P(DW_\infty, k_n, DW_0)}{\int P(d|DW_\infty, k_n, DW_0) P(DW_\infty, k_n, DW_0) \partial\theta}, \quad (9)$$

where P = the probability;
k_n = the growth parameter of the n model;
d = the data; and
$\partial\theta$ = the partial derivate for each parameter θ.

The complexity of this multiparameter equation requires numerical integration. Therefore, we used a Markov chain Monte Carlo algorithm to obtain the posterior probability distribution by drawing random samples from the vector of all parameters of each model. For this purpose, we used JAGS, assuming an additive error. To assess the posterior distribution convergence, 4 Markov chains were simulated, with 100,000 iterations, a burn-in of 5000 runs, and a thinning of 1 iteration (Carrillo-Colín et al., 2021). Trace plots were assessed visually (Gelman and Rubin, 1992).

Model selection

To decide which model best explained and predicted the growth of round stingrays with Markov chain Monte Carlo numerical integration, we used the WAIC. This Bayesian criterion considers the entire parameter's likelihood matrix (Watanabe, 2009). First, model selection was made after comparing the WAIC values of the 3 competing models, and the one with the lowest WAIC value was selected. After that, the selected model, including the version with

Table 1

Reported growth parameters for male (M) and female (F) round stingray (*Urobatis halleri*) or for both sexes combined from other studies. These published means for disc width at birth (DW_0), theoretical maximum disc width (DW_∞), and the growth coefficient (k) were used in this study to set the parameters of the prior distributions and to compare the von Bertalanffy growth function (VBGF) and the Gompertz growth model for round stingray in the southern Gulf of California in Mexico. A single asterisk (*) indicates a value of DW_∞ determined through the transformation of the theoretical maximum total length (TL_∞) of 47.2 cm with the equation DW=1.33+0.53(TL) obtained in this study. A double asterisk (**) indicates values for the completion growth parameter from the Gompertz growth model. A dash indicates that the k value was not provided by the author.

Model	Sex	DW_∞ (cm)	DW_0 (cm)	k (year^{-1})	Location of study	Source
VBGF	F	31.00	7.50	–	Seal Beach, California	Babel (1967)
	M	25.00	7.50	–		
VBGF	Both	26.35*	4.72	0.27	Gulf of California, Mexico	Morales-Azpeitia et al. (2013)
VBGF	F	22.45	7.60	0.15	Seal Beach, California	Hale and Lowe (2008)
	M	28.56	7.50	0.09		
Gompertz	F	46.56	7.00	0.16**	Southern Gulf of California, Mexico	Diliegros-Valencia (2019)
	M	30.75	7.00	0.26**		

sex variation, was fitted, and the WAIC was computed. The WAIC values of the selected model for both sexes (reduced model) and its version that includes sex variation (full model) were then compared to decide if there was evidence of differences in growth between sexes.

Results

In total, 244 round stingrays were examined (99 females and 145 males). We found weak evidence (BF_{10}=1.00) in the mean differences in DW between sexes, where males were 1.01 cm (SD 0.50) larger than females (95% credible interval [CI]: 0.03–2.01). The size range for sexes combined was 7.8–24.5 cm DW (mean: 14.36 cm DW [SD 3.87]) (Fig. 1). We found conclusive evidence (BF_{10}>100) of a positive linear correlation between DW and VD (coefficient of determination [r^2]=0.87) with regression coefficients a and b of 18.43 (95% CI: 12.04–24.74) and 55.26 (95% CI: 52.62–58.03), respectively, described by the equation DW=18.43+55.26(VD) for sexes combined (Fig. 2).

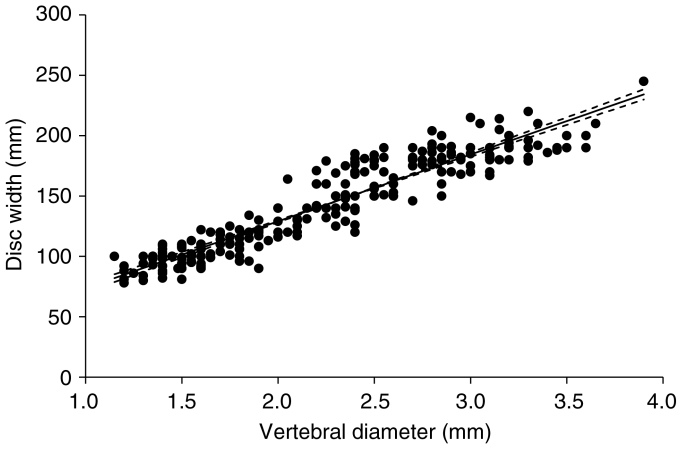

Figure 2

Relationship between vertebral diameter and disc width for round stingrays (*Urobatis halleri*) sampled during 2007–2012 in the southern Gulf of California in Mexico (for sexes combined). Dashed lines indicate the 95% credible interval.

Growth-band counts ranged from 0 to 8. The 3 readers agreed on 38% of the counts. When just 2 readers agreed (62% of cases), their count differed by 1 band in 59% of cases and by 2 bands in 3% of cases. The indicators of bias and precision for the total sample were as follows: IAPE=20%, CV=27%, and D=56%. Visual inspection of the age-bias plots between each pair of readers revealed minimal variation around the 1:1 ratio (Fig. 3, A–C). The results of the post hoc tests done as part of the ANOVA provide anecdotal evidence that the mean counts between readers 1 and 2 were different (BF_{10}=2.02). In contrast, for the mean counts between readers 1 and 3 (BF_{10}=0.27) and readers 2 and 3 (BF_{10}=0.17), the evidence of difference was null (Fig. 3D).

Results from the CEA indicate that the highest frequency of opaque edges occurred in the summer months, likely the time when deposition of growth bands began. Results from the MIA indicate that growth-band deposition appears close to being completed in November–December when the maximum MI was reached (Fig. 4). The lower MI estimated in the fourth bimester (July–August) was probably caused by the low sample size. However, we found substantial evidence in the mean differences in MI between bimester 2 (March–April) and bimester 4 (July–August), bimester 3 (May–June) and bimester 4 (July–August), and bimester 5 (September–October) and bimester 6 (November–December) (Suppl. Table). Results from both CEA and MIA indicate that every growth band was formed annually.

The estimated ages for sexes combined ranged from 0 to 8 years. The mean age of all the samples was 2.27 years (SD 1.87), with 23.8% and 17.6% of individuals aged at 0 and 1 years, respectively. As it is with many elasmobranchs, overlap in size at age increased with age for our specimens of the round stingray, which can be seen in the size-at-age key in Table 2.

The model selected according to the WAIC as the best fit to the data was the VBGF (Table 3). When sex was included in the VBGF, the WAIC increased by 6.46 units (from 804.47 to 810.93). Given the loss of parsimony by including sex as

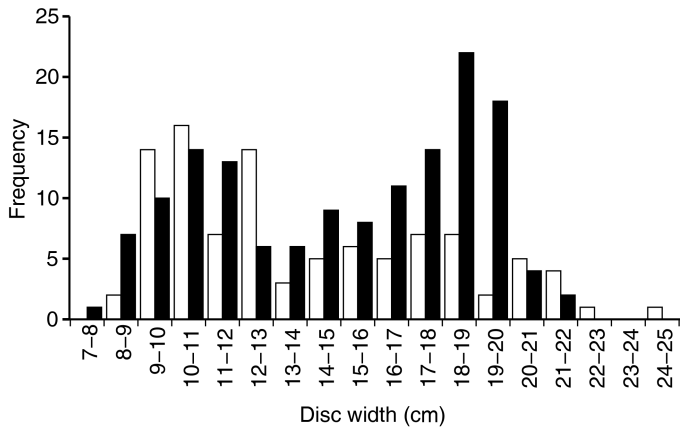

Figure 1

Length–frequency distributions for female (white bars) and male (black bars) round stingrays (*Urobatis halleri*) sampled during 2007–2012 in the southern Gulf of California in Mexico (number of rays=244).

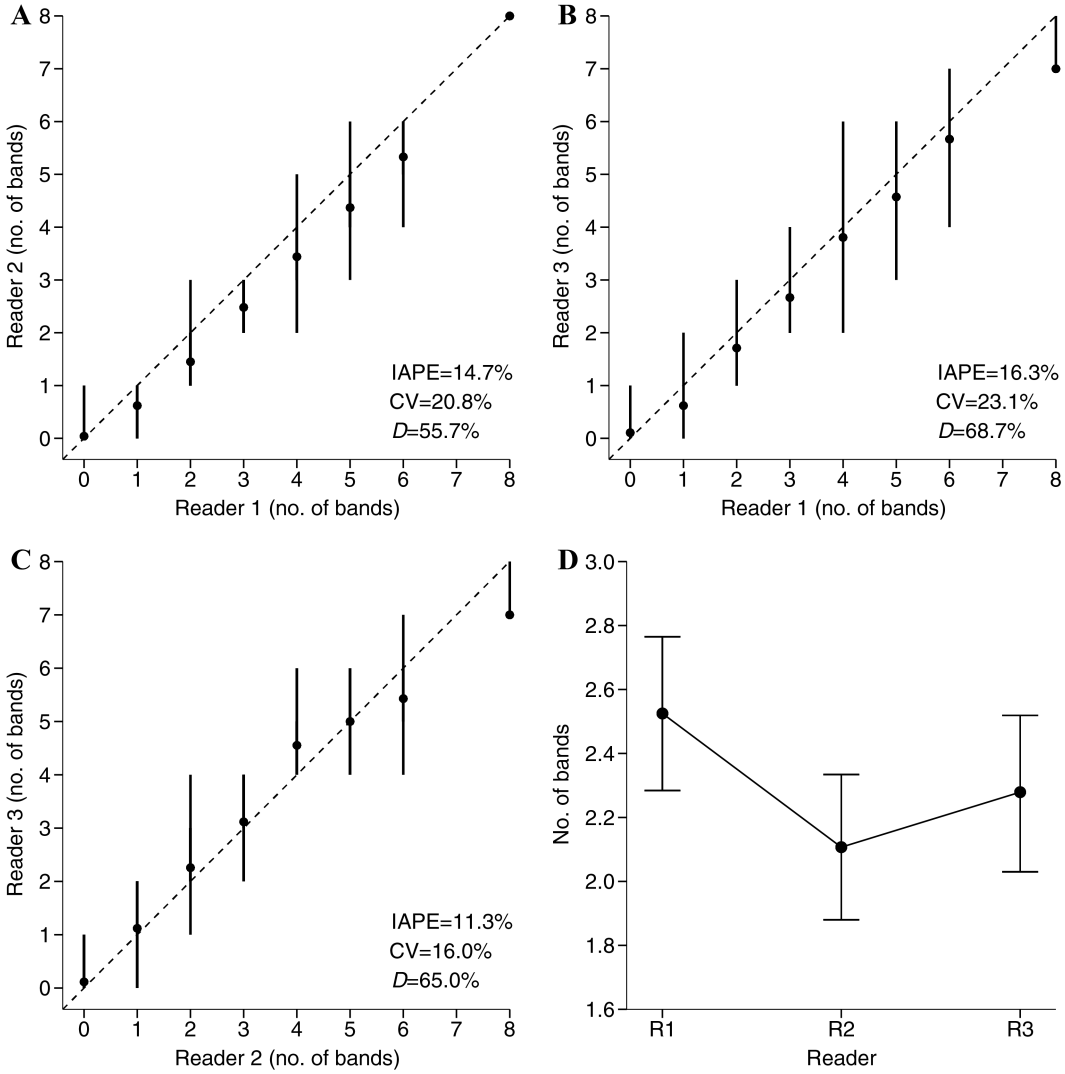

Figure 3

Age-bias plots of counts of growth bands on vertebrae of round stingrays (*Urobatis halleri*) sampled between 2007 and 2012 in the southern Gulf of California in Mexico. Black circles represent mean counts (**A**) of reader 2 (R2) relative to reader 1 (R1), (**B**) of reader 3 (R3) relative to reader 1, (**C**) of reader 3 relative to reader 2, and (**D**) between readers 1–3 from ad hoc Bayesian one-way analysis of variance. Error bars represent the range of band counts assigned by readers. The dashed line in panels A–C indicate 1:1 equivalence. Reproducibility and precision of age estimates were assessed by using the index of average percent error (IAPE), coefficient of variation (CV), and precision index (*D*).

a factor, we selected the VBGF fitted with data for the sexes combined. The mean values of marginal posteriors from the VBGF were as follows: DW_0=9.52 cm (95% CI: 9.25–9.79), DW_∞=32.50 cm (95% CI: 30.60–34.46), and k=0.114 year^{-1} (95% CI: 0.101–0.129). The growth curve is monotonic as expected. However, because the sample size decreased with age, the model lost accuracy at ages 6 and 8 (Fig. 5). The VBGF for the round stingray predicts growth from the birth size of 9.52 cm DW to 11.92 cm DW for age 1 and to 14.21 cm DW for age 2. Therefore, the growth rate from age 0 to age 1 and age 2 was 2.48 cm/year and 2.21 cm/year, respectively.

The marginal posterior probability distribution of the VBGF parameters (Fig. 6) indicates a smooth and well-defined shape for every parameter (Fig. 6, A, C, E). The relationship of DW_∞ to k is typically inverse (Fig. 6B). Similarly, the relationship of k to DW_0 is inverse but with a slope that is less steep (Fig. 6F), whereas the relationship of DW_0 to DW_∞ is dispersed and centered without correlation (Fig. 6D).

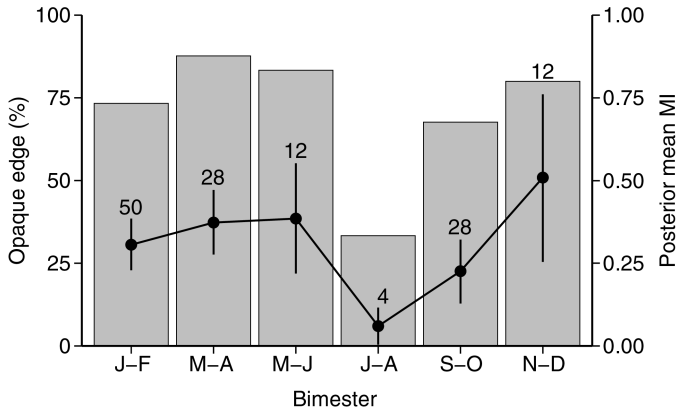

Figure 4

The periodicity of band formation was assessed by using marginal increment (MI) analysis and edge percentage analysis for round stingrays (*Urobatis halleri*) sampled during 2007–2012 in the southern Gulf of California in Mexico. The black circles represent the posterior mean marginal increments, and the error bars indicate the 95% credible intervals. The gray columns represent the percentages of opaque edges. Numerals above the circles indicate number of rays. Results of analyses are shown for each bimester (2-month interval): January–February, March–April, May–June, July–August, September–October, and November–December.

Discussion

The maximum age of the round stingray found in this study (8 years) is the same as that found by Babel (1967) but lower than that reported by Hale and Lowe (2008) (14 years). Furthermore, the latter authors found statistical differences in growth between males and females. This difference could be related to the size structure of both samples. Although the size range obtained in this study is similar to that in the study by Hale and Lowe (2008), their sample was composed mainly of males (71%), and our sample did not have such bias in sex proportion (59% males). Differences in availability could produce the phenomenon of apparent change in the growth rate like gear selectivity can (Walker et al., 1998). Also, the difference in conclusions between the studies could be a result of the use of the different statistical approach in our study (Gerrodette, 2011).

Compared to other members of the family Urotrygonidae, the round stingray has a maximum age that is similar to that of the Panamic stingray (*Urotrygon aspidura*) from the Pacific coast of Columbia (Torres-Palacios et al., 2019) but is shorter than that reported for the

Table 2

Age–size key for round stingrays (*Urobatis halleri*) sampled between 2007 and 2012 in the southern Gulf of California in Mexico (for sexes combined). In the center of the table are the numbers of individuals that correspond to each disc width (DW) class and age class. In the margin of the table, the total number of stingrays (*n*) and the mean and standard deviation (SD) for each DW class and age class are presented.

	Age (years)											
DW (cm)	0	1	2	3	4	5	6	7	8	*n*	Mean (years)	SD
7–8	1									1	0.0	–
8–9	9									9	0.0	–
9–10	22	2								24	0.1	0.28
10–11	21	9								30	0.3	0.47
11–12	4	13	3							20	1.0	0.60
12–13	1	12	7							20	1.3	0.57
13–14		4	5							9	1.6	0.53
14–15		3	8	3						14	2.0	0.68
15–16			8	6						14	2.4	0.51
16–17			5	10	1					16	2.8	0.58
17–18			1	12	7		1			21	3.4	0.81
18–19				4	15	8	2			29	4.3	0.80
19–20				1	8	7	4			20	4.7	0.86
20–21					3	4	2			9	4.9	0.78
21–22					1	3	2			6	5.2	0.75
22–23						1				1	5.8	–
24–25									1	1	8.0	–
n	58	43	37	36	35	23	11		1	244		
Mean (cm)	9.7	11.7	14.0	16.6	18.5	19.4	19.4		–	14.4	2.3	
SD	0.89	1.19	1.55	1.32	0.95	1.20	1.17		–	3.96		1.87

Table 3

Comparison of the von Bertalanffy, Gompertz, and logistic growth models fit to length-at-age data for round stingrays (*Urobatis halleri*) sampled between 2007 and 2012 in the southern Gulf of California in Mexico. The parameters are disc width at birth (DW_0, in centimeters), theoretical maximum length (DW_∞, in centimeters), and the growth coefficient (k, year^{-1}) for the von Bertalanffy growth function and the completion growth coefficient (k_2, year^{-1}) for the Gompertz and logistic growth models. Posterior values and 95% credible intervals (lower quartile: 2.5%; upper quartile: 97.5%) are provided from the fit of the growth models with a Markov chain Monte Carlo algorithm to data pooled for both sexes. The Watanabe–Akaike information criterion (WAIC) was used in model selection. The deviance information criterion (DIC) is reported to facilitate comparison of parameter estimates with those from previous studies in which the frequentist approach was used. SD=standard deviation; SE=standard error.

				Credible interval			
Model	Parameter	Mean	SD	2.5%	97.5%	DIC	WAIC (SE)
von Bertalanffy						805.20	804.47 (20.3)
	DW_0	9.52	0.14	9.25	9.79		
	DW_∞	32.55	0.97	30.60	34.46		
	k	0.11	0.01	0.10	0.13		
	SD	1.25	0.06	1.15	1.37		
Gompertz						824.10	820.77 (21.1)
	DW_0	9.80	0.13	9.55	10.06		
	DW_∞	33.64	1.03	31.65	35.70		
	k_2	0.17	0.01	0.15	0.18		
	SD	1.30	0.06	1.19	1.42		
Logistic						898.30	897.75 (21.5)
	DW_0	11.71	0.17	11.38	12.04		
	DW_∞	34.82	1.01	32.84	36.77		
	k_2	0.15	0.01	0.14	0.16		
	SD	1.52	0.07	1.30	1.66		

blotched stingray (*Urotrygon chilensis*) (14 years) in the Mexican Pacific Ocean (Guzmán Castellanos, 2015). This new information about the maximum age of the round stingray has considerable implications for studies of population dynamics.

The evidence of a relationship between VD and DW supports the use of vertebrae for aging (Goldman et al., 2012). The precision values (IAPE, CV, D) for samples in our study are within the expected interval for this group of species (Campana, 2001) and agree with the readings that have been done for the family Urotrygonidae (Mejía-Falla et al., 2014; Guzmán Castellanos, 2015; Santander Neto, 2015; Diliegros-Valencia, 2019).

Results from both the CEA and MIA support the assumption of an annual pattern of growth-band formation, and annual formation has also been reported for round stingrays in California (Hale and Lowe, 2008) and in the southeastern

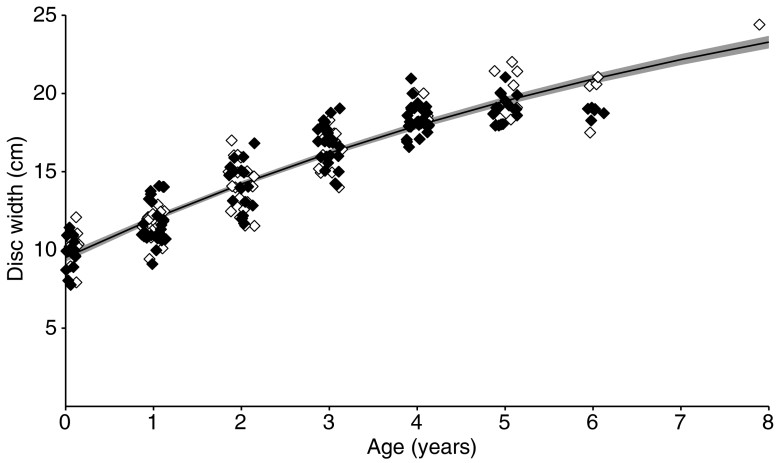

Figure 5

Estimated von Bertalanffy growth curve for round stingrays (*Urobatis halleri*) in the southern Gulf of California in Mexico (for sexes combined). The black (male) and open (female) diamonds represent observed lengths at age for stingrays sampled during 2007–2012. The gray shaded area indicates the 95% credible interval.

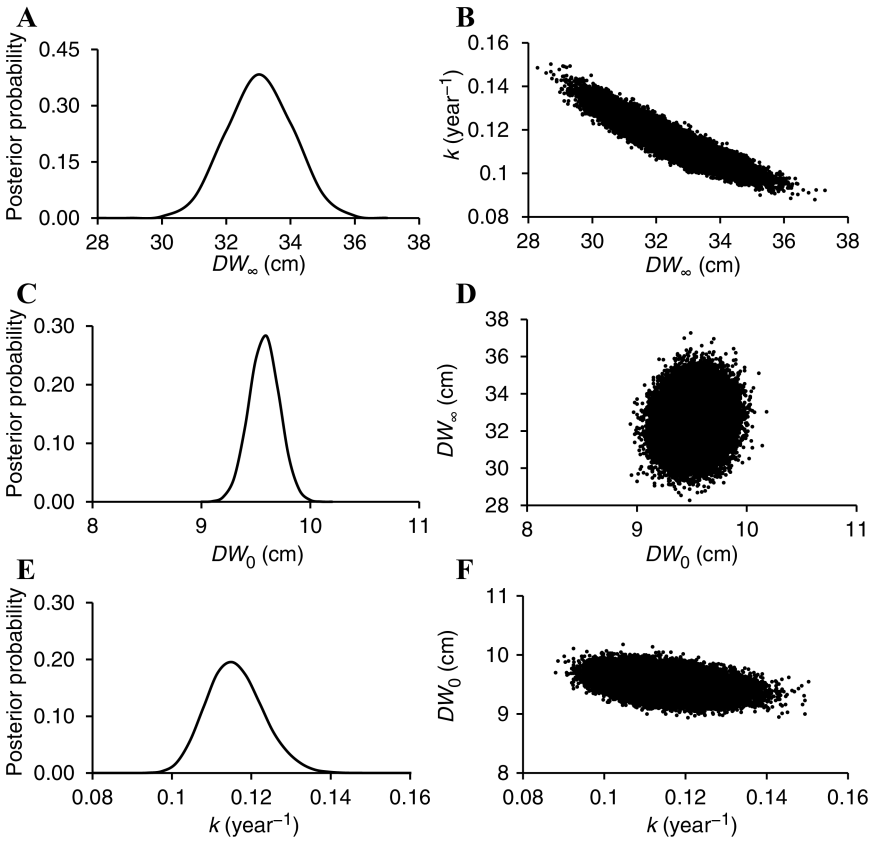

Figure 6

The Bayes posterior probability distributions of the (**A**) theoretical maximum disc width (DW_∞), (**C**) disc width at birth (DW_0), and (**E**) growth coefficient (k), the parameters of the von Bertalanffy growth function, paired with scattergrams of the relationships between the model's parameters, (**B**) DW_∞ to k, (**D**) DW_0 to DW_∞, and (**F**) k to DW_0. Values are predicted from the 100,000 Markov chain Monte Carlo simulations used to fit the von Bertalanffy growth function to observed length-at-age data for round stingrays (*Urobatis halleri*) sampled during 2007–2012 in the southern Gulf of California in Mexico.

GOC (Diliegros-Valencia, 2019). The opaque bands were deposited in the summer months. They are broad and represent rapid growth, and the translucent bands formed in winter are thinner and reflect slower growth (Cailliet et al., 1986; Cailliet and Goldman, 2004). Evidence of variability between individuals in the number of band pairs has been documented for the round stingray (James and Natanson, 2020), and such a source of bias was prevented in this study by using just the cervical vertebrae for all round stingrays. Also, band-pair counts without validation need to be taken with caution. Although there are more direct methods for validating the periodicity of growth bands of aquatic organisms, CEA and MIA are advantageous because they yield reliable and comparable results (Campana, 2001; Carrillo-Colín et al., 2021). Although new methods and approaches will rise to overcome the current controversies in age studies for batoids (James and Natanson, 2020), our statistical approach and results set a baseline for the age and growth of the round stingray in the tropical region of the Pacific Ocean.

In this study, we explored 3 conceptually different models that include DW_0, an appropriate parameter for viviparous chondrichthyans (Cailliet et al., 2006). We avoided exploring other models with more parameters because the WAIC penalizes them or because they do not have any biological significance (Richards, 1959; Katsanevakis, 2006). The continuous growth pattern observed in this study (as indicated by parameter estimates from the VBGF) and the representativeness of most age groups indicate that the round stingray completes its life cycle in the study area (Bergstad et al., 2021). Interestingly, the round stingray has been reported to segregate by size and life stage (Silva-Garay and Lowe, 2021), but there are no signs of segregation in our data set. Size segregation and

length selectivity of fishing gears can bias growth data to indicate a discontinuous pattern (Walker et al., 1998) that can favor more flexible models (with an inflection point) or even 2-phase growth models arguing investment in reproductive processes (Torres-Palacios et al., 2019).

The round stingray is not commercially targeted in the GOC artisanal fisheries (Bizzarro et al., 2009). However, the low sample size for large individuals (>6 years and >22 cm DW) might indicate an effect of fishing mortality on its population due to being caught as bycatch of shrimp trawlers (Garcés-García et al., 2020), as implied by the difference between the observed maximum DW (24.50 cm) and the estimated mean DW_∞ (32.50 cm). Fortunately, the statistical framework used in this study allowed us to estimate DW_∞ by combining the prior information and support of data considering the parameter's uncertainty in a probabilistic manner.

Size selectivity does not seem to be an explanation for the absence of large individuals because the maximum DW obtained during this study is very similar to those of other studies (27.00 cm; Hale and Lowe, 2008), and such a minimal difference in maximum DW does not indicate a significant difference in swimming speeds or turning ability. The latter may be true for species with higher swimming ability and size, such as the golden cownose ray (*Rhinoptera steindachneri*), the eagle rays (*Myliobatis* spp.), or those of the genus *Hypanus*, which are more likely to outswim the relatively slow shrimp trawls. In contrast, the poor mobility of round stingrays limits their ability to escape, and their flattened shape restricts size selection through the trawl. Consequently, fishing mortality is likely to affect the size range of the round stingrays available in the fishing area and susceptible to being captured by the trawlers. Although our surveys were conducted with small trawl nets used in the artisanal shrimp fishery, the size range sampled was convenient for this study and included individuals in all classes for both sexes. Furthermore, similar sizes for the round stingray were recently reported from fishery-independent surveys conducted with large vessels and in different areas, depths, and seasons in the GOC (Garcés-García et al., 2020).

In this study, we investigated the round stingray's age and growth and developed a fully Bayesian approach for estimation of all quantities. In contrast, leaving the model fitting to the data alone could produce misleading estimates of parameters, especially when the observed data do not follow the expected pattern, are incomplete, or are biased. The stochastic approach in which Monte Carlo simulation is used can be advantageous for remedying the lack of fit. However, it also requires assigning a probability distribution to the parameters without weighting them with the data to produce the final distributions of the parameters (Neer et al., 2005). Alternatively, the Bayesian approach in this study relies on the explicit use of uncertainty for the growth parameters. A parameter's uncertainty is expressed as a probability distribution and combined with the information contained in the data (likelihood) throughout the Bayes theorem (Equation 9); it is possible to obtain an enriched marginal posterior probability distribution (Fig. 6) of each parameter (Gelman et al., 2003). This fact is essential in age and growth studies when parameters can be informative based on the knowledge of the life history of a species, as is the case for DW_0 (Carrillo-Colín et al., 2021; Smart and Grammer, 2021).

Neither Monte Carlo simulation nor the Bayesian approach can correct for biases in the data caused by length-selective fishing mortality. Troynikov and Walker (1999) stated that the influence of length-selective mortality on determining growth parameters is not easily explained because it is a combination of 2 overlapping effects on lengths for different age classes. These authors proved that a growth pattern can be affected by an apparent change in growth rate due to length-selective fishing mortality.

Reporting the parameters as probability distributions (and their credible intervals) is not only fundamentally different from classical (frequentist) estimation but also useful as inputs in further quantitative demographic analysis or stock assessment for elasmobranchs (Cortés, 2002). However, the philosophy of measuring the statistical support of each growth parameter when fitting the model goes beyond the scope of our work described here (Gerrodette, 2011).

In our study, we used the Bayes factor in the *t*-test and ANOVA to evaluate the size of the effects, and we used the WAIC for the selection of the best growth models. The WAIC is convenient for more complex stochastic numerical approximations.

The convergence of the growth parameters DW_∞, k, and DW_0 was satisfactorily achieved on the basis of their marginal posterior distributions (Carrillo-Colín et al., 2021). The informative prior distribution for DW_0 favored model fitting because it helped in the selection of realistic birth size values (Rolim et al., 2020; Smart and Grammer, 2021). The k value (from the VBGF) we obtained in our study ranged between 0.11 and 0.13 year^{-1} and is close to the range of 0.2–0.5 year^{-1} that has been reported for species of the families Rhinobatidae, Torpedinidae, and Urotrygonidae (Cailliet and Goldman, 2004). However, it must be noted that this broad difference in k values can also be related to sample size, aging method, and verification, validation, and growth model fitting techniques (Cailliet and Goldman, 2004).

Conclusions

In the GOC, chondrichthyan populations have long been affected by fisheries that trawl for teleost and shrimp species. Capture as bycatch in those fisheries causes significant mortality for species of no commercial value, including for the round stingray and other demersal small rays (Garcés-García et al., 2020). Variations in life-history characteristics among populations can be expected in chondrichthyan species because of the following: 1) cold-water species tend to grow larger and

probably live longer than tropical water species; 2) differences in food availability, habitat type, and environmental conditions affect their growth rate; and sample distribution can be biased 3) by the effects of migration and segregation and 4) by the length selectivity of fishing gears (Walker, 1998; Walker et al., 1998). In this study, we estimated growth parameters by using the counts of growth bands in vertebrae taken from sampled round stingrays. We found a maximum age of 6 or 8 years, a remarkably short life span for a chondrichthyan species, indicating that the round stingray has a short intrinsic generation time and, therefore, a high intrinsic rate of population increase (King and McFarlane, 2003). Stock assessment and ecological risk analyses require inputs from age, growth, and reproductive rate studies. The Bayesian estimation of this study can be used in future quantitative analyses to gain the advantage of considering uncertainty in the estimation of parameters (Punt and Hilborn, 1997).

Resumen

Los estudios sobre la historia de vida de las especies descartadas en pesquerías son de baja prioridad, especialmente aquellos sobre estimaciones de edad y crecimiento. En consecuencia, se desconoce casi todo sobre estas especies, a pesar de haber sido capturadas de forma incidental por mucho tiempo. En este estudio, las estimaciones de edad se obtuvieron utilizando las vértebras de la raya redonda (*Urobatis halleri*). Se ajustaron 3 diferentes modelos de crecimiento (von Bertalanffy, Gompertz y logístico) a datos de longitud a la edad. La estimación Bayesiana de los distintos parámetros de crecimiento se realizó mediante el algoritmo cadenas de Markov de Monte Carlo. Se incluyeron y consideraron distribuciones previas informativas de los parámetros ancho del disco al nacer (DW_0) y ancho del disco máximo teórico (DW_∞). Las distribuciones previas para el coeficiente de crecimiento (k) y el parámetro de terminación del crecimiento (k_2) se establecieron como no informativas (k para la función de crecimiento de von Bertalanffy y k_2 para los modelos de crecimiento Gompertz y logístico). Los resultados de nuestros análisis indican que las bandas de crecimiento son anuales y que la raya redonda vive hasta 8 años. Según el criterio de información de Watanabe–Akaike para la selección del modelo, la función de crecimiento de von Bertalanffy para sexos combinados fue seleccionada como el mejor modelo. Los valores promedio de las posteriores marginales fueron los siguientes: DW_0=9.52 cm (intervalo de credibilidad [IC] al 95%: 9.25–9.79), DW_∞=32.50 cm (IC 95%: 30.60–34.46), y k =0.114 año^{-1} (IC 95%: 0.101–0.129).

Acknowledgments

We express our gratitude to T. Walker for his constructive review and recommendations. This research was funded by Universidad Autónoma de Sinaloa through the projects PROFAPI-UAS (81-2010) and PROFAPI-UAS (101-2011).

Literature cited

Babel, J. S.
1967. Reproduction, life history and ecology of the round stingray *Urolophus halleri* Cooper. Calif. Dep. Fish Game, Fish Bull. 137, 104 p.

Bergstad, O. A., R. H. Hunter, N. J. Cousins, D. M. Bailey, and T. Jørgensen.
2021. Notes on age determination, size and age structure, longevity and growth of co-occurring macrourid fishes. J. Fish Biol. 99:1032–1043. Crossref

Bizzarro, J. J., W. D. Smith, J. F. Márquez-Farías, J. Tyminski, and R. E. Hueter.
2009. Temporal variation in the artisanal elasmobranch fishery of Sonora, Mexico. Fish. Res. 97:103–117. Crossref

Cailliet, G. M.
2015. Perspectives on elasmobranch life-history studies: a focus on age validation and relevance to fishery management. J. Fish Biol. 87:1271–1292. Crossref

Cailliet, G. M., and K. J. Goldman.
2004. Age determination and validation in chondrichthyan fishes. *In* Biology of sharks and their relatives (J. C. Carrier, J. A. Musick, and M. R. Heithaus, eds.), p. 399–447. CRC Press, Boca Raton, FL.

Cailliet, G. M., R. L. Radtke, and B. A. Welden.
1986. Elasmobranch age determination and verification: a review. *In* Indo-Pacific fish biology: proceedings of the second international conference on Indo-Pacific fishes (T. Uyeno, R. Arai, T. Taniuchi, and K. Matsuura, eds.), p. 345–360. Ichthyol. Soc. Jpn., Tokyo, Japan.

Cailliet, G. M., W. D. Smith, H. F. Mollet, and K. J. Goldman.
2006. Age and growth studies of chondrichthyan fishes: the need for consistency in terminology, verification, validation, and growth function fitting. Environ. Biol. Fishes 77:211–228. Crossref

Campana, S. E.
2001. Accuracy, precision and quality control in age determination, including a review of the use and abuse of age validation methods. J. Fish Biol. 59:197–242. Crossref

Campana, S. E., M. C. Annand, and J. I. McMillan.
1995. Graphical and statistical methods for determining the consistency of age determinations. Trans. Am. Fish. Soc. 124:131–138. Crossref

Carrillo-Colín, L. D., J. F. Márquez- Farías, R. E. Lara-Mendoza, and O. G. Zamora-García.
2021. Bayesian estimation of the age and growth of the golden cownose ray (*Rhinoptera steindachneri*) in the southern Gulf of California in Mexico. Fish. Bull. 119:10–20. Crossref

CONAPESCA-INP (Comisión Nacional de Acuacultura y Pesca-Instituto Nacional de la Pesca).
2004. Plan de acción nacional para el manejo y conservación de tiburones, rayas y especies afines en México, 80 p. Com. Nac. Acuac. Pesca and Inst. Nac. Pesca, Secr. Agric. Ganad. Desarro. Rural Pesca Aliment., Mazatlán, Mexico. [Available from website.]

Cortés, E.
2002. Stock assessment of small coastal sharks in the U.S. Atlantic and Gulf of Mexico. Southeast Data Assess. Rev., SEDAR 13-DW-13, 133 p. [Available from website.]

Diliegros-Valencia, M.
2019. Edad y crecimiento de la raya redonda *Urobatis halleri* (Cooper, 1863) en el Sur de Sinaloa y Norte de Nayarit,

México. Bachelor's thesis, 69 p. Univ. Veracruzana, Tuxpan, Veracruz, Mexico.

Ebert, D. A.
2003. Sharks, rays and chimaeras of California, 297 p. Univ. Calif. Press, Berkeley, CA.

Garcés-García, K. C., J. Tovar-Ávila, B. Vargas-Trejo, D. A. Chávez-Arrenquín, T. I. Walker, and R. W. Day.
2020. Elasmobranch bycatch by prawn trawls in the Gulf of California: first comprehensive analysis and the effect of fish escape devices. Fish. Res. 230:105639. Crossref

Gelman, A. D., and D. B. Rubin.
1992. Inference from iterative simulation using multiple sequences. Stat. Sci. 7:457–472. Crossref

Gelman, A., J. B. Carlin, H. S. Stern, and D. B. Rubin.
2003. Bayesian data analysis, 2nd ed., 668 p. Chapman and Hall/CRC, London.

Gerrodette, T.
2011. Inference without significance: measuring support for hypotheses rather than rejecting them. Mar. Ecol. 32:404–418. Crossref

Goldman, K. J., and J. A. Musick.
2006. Growth and maturity of salmon sharks (*Lamna ditropis*) in the eastern and western North Pacific, and comments on back-calculation methods. Fish. Bull. 104:278–292.

Goldman, K. J., G. M. Cailliet, A. H. Andrews, and L. J. Natanson.
2012. Assessing the age and growth of Chondrichthyan fishes. *In* Biology of sharks and their relatives, 2nd ed. (J. C. Carrier, J. A. Musick, and M. R. Heithaus, eds.), p. 423–451. CRC Press, Boca Raton, FL.

Guzmán Castellanos, A. B.
2015. Historia de vida de la raya chilena *Urotrygon chilensis* (Günther, 1872) en el sureste del Pacífico mexicano. Ph.D. diss., 133 p. Cent. Investig. Biol. Noroeste, La Paz, Mexico. [Available from website.]

Hale, L. F., and C. G. Lowe.
2008. Age and growth of the round stingray *Urobatis halleri* at Seal Beach, California. J. Fish Biol. 73:510–523. Crossref

Hoisington, G., IV, and C. G. Lowe.
2005. Abundance and distribution of the round stingray, *Urobatis halleri*, near a heated effluent outfall. Mar. Environ. Res. 60:437–453. Crossref

James, K. C., and L. J. Natanson.
2020. Positional and ontogenetic variation in vertebral centra morphology in five batoid species. Mar. Freshw. Res. 72:887–898. Crossref

Jeffreys, H.
1961. Theory of probability, 3rd ed., 447 p. Oxford Univ. Press, Oxford, UK.

JASP Team.
2021. JASP. Computer software, vers. 0.15. [Available from website, accessed September 2021.]

Katsanevakis, S.
2006. Modelling fish growth: model selection, multi-model inference and model selection uncertainty. Fish. Res. 81:229–235. Crossref

Katsanevakis, S., and C. D. Maravelias.
2008. Modelling fish growth: multi-model inference as a better alternative to a priori using von Bertalanffy equation. Fish Fish. 9:178–187. Crossref

Kass, R. E., and A. E. Raftery.
1995. Bayes factors. J. Am. Stat. Assoc. 90:773–795. Crossref

King, J. R., and G. A. McFarlane.
2003. Marine fish life history strategies: applications to fishery management. Fish. Manag. Ecol. 10:249–264. Crossref

López-Martínez, J., E. Herrera-Valdivia, J. Rodríguez-Romero, and S. Hernández-Vázquez.
2010. Peces de la fauna de acompañamiento en la pesca industrial de camarón en el Golfo de California, México. Rev. Biol. Trop. 58:925–942.

Lluch-Cota, S. E., E. A. Aragón-Noriega, F. Arreguín-Sánchez, D. Aurioles-Gamboa, J. J. Bautista-Romero, R. C. Brusca, R. Cervantes-Duarte, R. Cortés-Altamirano, P. Del-Monte-Luna, A. Esquivel-Herrera, et al.
2007. The Gulf of California: review of ecosystem status and sustainability challenges. Prog. Oceanogr. 73:1–26. Crossref

Lyons, K., D. A. Ebert, and C. G. Lowe.
2015. *Urobatis halleri*. The IUCN Red List of Threatened Species 2015:e.T60108A80677446. [Available from website accessed January 2021].

Márquez-Farías, J. F.
2002. The artisanal ray fishery in the Gulf of California: development, fisheries research and management issues. Shark News 14:12–13.
2007. Reproductive biology of shovelnose guitarfish *Rhinobatos productus* from the eastern Gulf of California México. Mar. Biol. 151:1445–1454. Crossref
2020. Length at maturity of the Pacific angel shark (*Squatina californica*) in the artisanal elasmobranch fishery in the Gulf of California in Mexico. Fish. Bull. 118:359–364. Crossref

Márquez-Farías, J. F., and M. P. Blanco-Parra.
2006. Rayas. *In* Sustentabilidad y pesca responsable en México: evaluación y manejo (F. A. Sánchez, L. B. Moreno, I. M. Gómez-Humarán, R. S. Sansores, and C. R. Dávalos, eds.), p. 303–321. Inst. Nac. Pesca, Mexico City, Mexico.

McEachran, J. D., and G. Notarbartolo-di-Sciara.
1995. Peces Batoideos. *In* Guía FAO para la identificación de especies para los fines de la pesca. Pacifico centro-oriental. Volumen 2: vertebrados—parte 1 (W. Fischer, F. Krupp, W. Schneider, C. Sommer, K. E. Carpenter, and V. H. Niem, eds.), p. 745–792. FAO, Rome.

Mejía-Falla, P. A., E. Cortés, A. F. Navia, and F. A. Zapata.
2014. Age and growth of the round stingray *Urotrygon rogersi*, a particularly fast-growing and short-lived elasmobranch. PLoS ONE 9(4):e96077. Crossref

Morales-Azpeitia, R., J. López-Martínez, C. H. Rábago-Quiroz, M. O. Nevárez-Martínez, and E. Herrera-Valdivia.
2013. Growth and mortality rates of *Pseudupeneus grandisquamis* and *Urobatis halleri* bycatch species in the shrimp fishery. Hidrobiológica 23:386–393.

Morey, R. D., and J. N. Rouder.
2018. BayesFactor: computation of Bayes factors for common designs. R package, vers. 0.9.12-4.2. [Available from website, accessed December 2020.]

Musick, J. A.
1999. Ecology and conservation of long-lived marine animals. Am. Fish. Soc. Symp. 23:1–10.

Natanson, L. J., J. G. Casey, and N. E. Kohler.
1995. Age and growth estimates for the dusky shark, *Carcharhinus obscurus*, in the western North Atlantic Ocean. Fish. Bull. 93:116–126.

Natanson, L. J., G. B. Skomal, S. L. Hoffmann, M. E. Porter, K. J. Goldman, and D. Serra.
2018. Age and growth of sharks: do vertebral band pairs record age? Mar. Freshw. Res. 69:1440–1452. Crossref

Neer, J. A., B. A. Thompson, and J. K. Carlson.
2005. Age and growth of *Carcharhinus leucas* in the northern Gulf of Mexico: incorporating variability in size at birth. J. Fish Biol. 67:370–383. Crossref

Nordell, S. E.
1994. Observations of the mating behavior and dentition of the round stingray, *Urolophus halleri*. Environ. Biol. Fishes 39:219–229. Crossref

Plummer, M.
2003. JAGS: a program for analysis of Bayesian graphical models using Gibbs sampling. *In* Proceedings of the 3rd international workshop on distributed statistical computing (DSC 2003); Vienna, 20–22 March (K. Hornik, F. Leisch, and A. Zeileis, eds.), 10 p. [Available from website.]

Punt, A. E., and R. Hilborn.
1997. Fisheries stock assessment and decision analysis: the Bayesian approach. Rev. Fish Biol. Fish. 7:35–63. Crossref

R Core Team.
2021. R: a language and environment for statistical computing. R Foundation for Statistical Computing, Vienna, Austria. [Available from website, accessed April 2021.]

Rábago-Quiroz, C. H., J. López-Martínez, J. E. Valdez-Holguín, and M. O. Nevárez-Martínez.
2011. Distribución latitudinal y batimétrica de las especies más abundantes y frecuentes en la fauna acompañante del camarón del Golfo de California, México. Rev. Biol. Trop. 59:255–267.

Richards, F. J.
1959. A flexible growth function for empirical use. J. Exp. Bot. 10:290–300.

Rouder, J. N., P. L. Speckman, D. Sun, R. D. Morey, and G. Iverson.
2009. Bayesian *t* tests for accepting and rejecting the null hypothesis. Psychon. Bull. Rev. 16: 225–237. Crossref

Rolim, F. A., Z. A. Siders., F. P. Caltabellotta, M. M. Rotundo, and T. Vaske-Júnior.
2020. Growth and derived life-history characteristics of the Brazilian electric ray *Narcine brasiliensis*. J. Fish Biol. 97:396–408. Crossref

Saldaña-Ruíz, L. E., O. Sosa-Nishizaki, Z. Ramírez-Mendoza, M. A. Pérez-Miranda, F. I. Rocha-González, and M. C. Rodríguez-Medrano.
2016. Reconstrucción de capturas por especie de la pesca artesanal de rayas del Golfo de California, 1997–2014. Cienc. Pesq. 24:81–96.

Santander Neto, J.
2015. Dinâmica populacional da raia *Urotrygon microphthalmum* Delsman, 1941 no nordeste do Brasil. Ph.D. diss., 142 p. Univ. Fed. Pernambuco, Recife, Brazil. [Available from website.]

Silva-Garay, L., and C. G. Lowe.
2021. Effects of temperature and body-mass on the standard metabolic rates of the round stingray, *Urobatis halleri* (Cooper, 1863). J. Exp. Mar. Biol. Ecol. 540:151564. Crossref

Smart, J. J., and G. L. Grammer.
2021. Modernising fish and shark growth curves with Bayesian length-at-age models. PLoS ONE 16(2):e0246734. Crossref

Smart, J. J., A. Chin, A. J. Tobin, and C. A. Simpfendorfer.
2016. Multimodel approaches in shark and ray growth studies: strengths, weaknesses and the future. Fish Fish. 17:955–971. Crossref

Torres-Palacios, K., P. A. Mejía-Falla, A. F. Navia, V. H. Cruz-Escalona, R. Félix-Uraga, and C. Quiñonez-Velázquez.
2019. Age and growth parameters of the Panamic stingray (*Urotrygon aspidura*). Fish. Bull. 117:169–179. Crossref

Troynikov, V. S., and T. I. Walker.
1999. Vertebral size-at-age heterogeneity in gummy shark harvested off southern Australia. J. Fish Biol. 54:863–877. Crossref

Walker, T. I.
1998. Can shark resources be harvested sustainably? A question revisited with a review of shark fisheries. Mar. Freshw. Res. 49:553–572. Crossref

Walker, T. I., B. L. Taylor, R. J. Hudson, and J. P. Cottier.
1998. The phenomenon of apparent change of growth rate in gummy shark (*Mustelus antarcticus*) harvested off southern Australia. Fish. Res. 39:139–163. Crossref

Watanabe, S.
2009. Algebraic geometry and statistical learning theory, 284 p. Cambridge Univ. Press, Cambridge, UK.

Zamora-García, O. G.
2015. Identificación de un punto de referencia para el cierre de temporada con base en la captura incidental de la pesquería industrial de camarón del Alto golfo de California. M.S. thesis, 120 p. Univ. Nac. Aut. Mex., Mexico City, Mexcio. [Available from: website.]